Editors' Suggestion

Triplet Superconductivity from Nonlocal Coulomb Repulsion in an Atomic Sn Layer Deposited onto a Si(111) Substrate

Sebastian Wolf,[1] Domenico Di Sante,[2,3] Tilman Schwemmer,[4] Ronny Thomale,[4] and Stephan Rachel[1]
[1]School of Physics, University of Melbourne, Parkville, Victoria 3010, Australia
[2]Department of Physics and Astronomy, University of Bologna, 40127 Bologna, Italy
[3]Center for Computational Quantum Physics, Flatiron Institute, New York, New York 10010, USA
[4]Institut für Theoretische Physik und Astrophysik, Universität Würzburg, Am Hubland Campus Süd, Würzburg 97074, Germany

(Received 14 July 2021; accepted 29 March 2022; published 22 April 2022)

Atomic layers deposited on semiconductor substrates introduce a platform for the realization of the extended electronic Hubbard model, where the consideration of electronic repulsion beyond the on-site term is paramount. Recently, the onset of superconductivity at 4.7 K has been reported in the hole-doped triangular lattice of tin atoms on a silicon substrate. Through renormalization group methods designed for weak and intermediate coupling, we investigate the nature of the superconducting instability in hole-doped Sn/Si(111). We find that the extended Hubbard nature of interactions is crucial to yield triplet pairing, which is f-wave (p-wave) for moderate (higher) hole doping. In light of persisting challenges to tailor triplet pairing in an electronic material, our finding promises to pave unprecedented ways for engineering unconventional triplet superconductivity.

DOI: 10.1103/PhysRevLett.128.167002

Introduction.—Unconventional superconductivity is one of the most active and exciting fields of physics research. The discovery of high-temperature superconductivity in doped cuprate materials in 1986 [1] and in iron-based superconductors 20 yr later [2,3] mark most notable events and has continuously fueled the search for room-temperature superconductors. Similarly, inherent topological superconductivity [4–7] has recently gained high importance, as the quasiparticles at zero energy (referred to as Majorana zero modes) exhibit non-Abelian braiding statistics [8], rendering them promising candidates for topological qubits and fault-tolerant quantum computing [9]. Note that, in order to narrow down the meaning of topological superconductors that is henceforth implied in this manuscript, it should be distinguished from proximity-induced topological superconductors, where, in general, a conventional superconductor induces topological pairing in an adjacent spin-orbit-coupled electron liquid [10–14]. The list of candidate materials for inherent topological superconductivity as a potential Majorana platform is rather short. This is because, at least at a moderate level of sophistication where one intends to accomplish an odd number of vortex core Majorana zero modes, one is primarily interested in chiral triplet superconductors, which as a predominant initial challenge brings about the task to identify triplet pairing candidate materials in the first place. Examples which have attracted much attention lately are $CePt_3Si$ [15,16], $Cu_xBi_2Se_3$ [17,18], $FeSe_{0.45}Te_{0.55}$ [19–21], and UTe_2 [22]. The most prominent example, however, had been Sr_2RuO_4 [23]—for decades the prime candidate for p-wave superconductivity. Yet, only recently, it was realized that the Knight shift evidence in favor of triplet pairing had to be reconsidered, now favoring singlet pairing [24] which, in order to comply with the other experimental evidence for strontium ruthenate, has to be described by a two-component complex order parameter [25–27].

Two-dimensional atom lattices on semiconductor substrates are a material platform with a rather simple electronic structure. The adsorption of only 1/3 monolayer of group-IV elements such as Pb and Sn forms a $(\sqrt{3}\times\sqrt{3})R30°$ structure, realizing a triangular lattice. Three out of four of the adatoms' valence orbitals are engaged in covalent back bonds with the substrate, leaving the fourth orbital as a half-filled dangling bond. As a consequence for the electronic structure, a single metallic surface band is present within the substrate's band gap. Such a half-filled surface band is subject to significant electron-electron interactions. For some of these materials, the presence of non-negligible nonlocal Coulomb interactions was suggested as the driving mechanism for their charge-ordered ground states [e.g., in Pb/Ge(111), Sn/Ge(111), or Pb/Si(111) [28–32]]. For Sn/Si(111), it was shown in angle-resolved photoemission spectroscopy (ARPES) that the observed band folding was deemed consistent with an antiferromagnetic ordering of the Sn lattice, in agreement with theoretical modeling of a Mott insulator [33]. Soon after, it was also argued that a Slater-type insulator might be the source of the observed magnetism [34]. In Ref. [35], spectral weight transfer as well as the formation of a quasiparticle peak was demonstrated experimentally, establishing the Mott picture. Moreover, nonlocal Coulomb interactions seem to be non-negligible and play an important role in Sn/Si(111) [29,30]. Most recently, the onset of

superconductivity at 4.7 ± 0.3 K has been observed in strongly boron-doped Sn/Si(111) [36]. The hole-doped silicon substrate was grown first, and the tin surface layer was deposited afterward, keeping the perfect triangular structure of the tin lattice. Doping levels of up to 10% could be reached. A sharp tunneling dip near zero bias is observed for low temperatures, compatible with a superconducting gap. It is further shown that the gap can be suppressed with increasing magnetic field strength. Detailed analysis of the superconducting gap deviates from conventional BCS behavior, hinting at the unconventional character of the pairing state [36], in agreement with the Mott insulating state of the undoped material [33]. The results reproduce many features of the correlated electron physics seen in complex oxides such as high-T_c square lattice cuprate superconductors. In contrast to cuprates, Sn/Si(111) is much simpler, both chemically and electronically, and would, thus, provide the cleanest platform for studying superconductivity emerging from a doped Mott insulator [37].

In this Letter, we investigate the competing pairing channels of correlated electrons in Sn/Si(111). By applying the weak-coupling renormalization group (WCRG) method, we are able to find the leading superconducting instabilities in an analytically controlled way in the limit of weak interactions. While correlated electrons on a hexagonal lattice have a generic propensity toward chiral d-wave pairing [38–46], we find that the Fermi surface (FS) structure of Sn/Si(111) leads to a competition between singlet and triplet pairing channels. The inclusion of nonlocal Coulomb interactions strongly suppresses the chiral d-wave state and instead favors f-wave and chiral p-wave triplet pairing. We further substantiate our findings by an intermediate-coupling analysis through functional renormalization group (FRG) calculations [47,48]; in addition, we can test competing ordering tendencies and rule out other many-body instabilities. From the synopsis of all results, we find that significant hole doping in combination with significant nonlocal Coulomb interactions—as proposed earlier [29,30]—might stabilize topologically nontrivial chiral p-wave pairing in Sn/Si(111).

Model and method.—We assume that boron-doped Sn/Si(111) is well described by an extended Hubbard model on the triangular lattice. The electronic band structure is derived from *local density approximation* (LDA) first-principle calculations [29,30,33], resulting in a single metallic band well separated from other bands. A tight-binding fit to the LDA band yields hopping terms up to fourth-nearest neighbors, $\mathcal{H}_0 = \sum_{ij} t_{ij} c^\dagger_{i\sigma} c_{j\sigma}$ and $t_{ij} \equiv t_{|j-i|}$; the band structure reads

$$\begin{aligned}\varepsilon_{\mathbf{k}} = &-2t_1[\cos k_x + 2\cos\sqrt{3}/2k_y \cos k_x/2] - 2t_2[\cos\sqrt{3}k_y + 2\cos 2/3k_x \cos\sqrt{3}/2k_y] - 2t_3[\cos 2k_x + 2\cos k_x \cos\sqrt{3}/2k_y] \\ &- 4t_4[\cos 5/2k_x \cos\sqrt{3}/2k_y + \cos 2k_x \cos\sqrt{3}k_y + \cos k_x/2 \cos 3\sqrt{3}/2k_y] \end{aligned} \quad (1)$$

with $t_1 = -52.7$ meV and $t_2/t_1 = -0.389$, $t_3/t_1 = 0.144$, and $t_4/t_1 = -0.027$ [30] (see Sec. III in Supplemental Material [49] for a discussion about variations of the hopping amplitudes). The band structure along the high-symmetry path is shown in Fig. 1(a) along with its contour plot in the Brillouin zone in Fig. 1(b), where constant-energy lines correspond to the FSs at different fillings. For comparison, Fig. 1(c) displays the analogous plot for an isotropic, nearest-neighbor triangular lattice.

The extended Hubbard Hamiltonian is given by

$$\mathcal{H} = \mathcal{H}_0 + U_0 \sum_i n_{i\uparrow} n_{i\downarrow} + U_1 \sum_{\langle ij \rangle} n_i n_j, \quad (2)$$

with $n_{i\sigma} \equiv c^\dagger_{i\sigma} c_{i\sigma}$, $n_i \equiv n_{i\uparrow} + n_{i\downarrow}$, and the local (nearest-neighbor) Hubbard interaction strength U_0 (U_1). Longer-ranged interactions are generically present but are often screened and, hence, mostly assumed subdominant by comparison to U_0. Notably, the situation is different for several group-IV adsorbates on semiconductor substrates, many of which possess charge-ordered ground states, which likewise tend to be favored by long-range

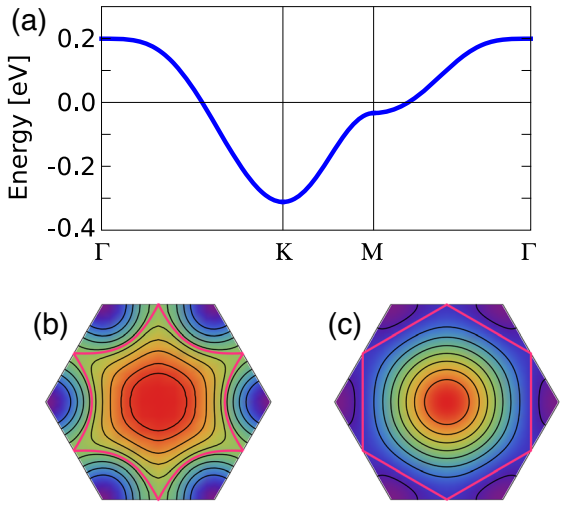

FIG. 1. (a) Tight-binding band structure (1) for Sn/Si(111). Fermi surfaces for different fillings are shown for Sn/Si(111) (b) and for the nearest-neighbor triangular lattice (c) as black lines. The van Hove fillings are shown in pink.

Coulomb repulsion [29,30]. Sn/Si(111) features a homogeneous charge distribution but instead orders magnetically, albeit with significant nonlocal Coulomb interaction being present [50]: The strongest spectral weight of the single-particle spectral function as measured in ARPES is shifted from the K to and beyond the M point [50], as observed in experiments [33] and in agreement with previous theoretical work [29]. The experimental data are best described by assuming a ratio of nearest-neighbor and local Hubbard interactions $1/3 \leq U_1/U_0 \leq 1/2$ [29,30]. This appears to be reasonable, and we will consider these parameters for the remainder of this work [51].

We investigate the superconducting instabilities and form factors of the model Hamiltonian (2) for the hole-doped case by virtue of the WCRG method [52–58] which builds upon the pioneering work of Kohn and Luttinger [59]. The main idea is to remain in a regime where a renormalized interaction near the FS can be safely calculated, which can be accomplished by sufficiently small interactions. A standard renormalization group procedure [60] is applied for the remaining effective degrees of freedom, where the weak-coupling approximation highlights the renormalization of couplings in the Cooper channel, since superconductivity generically is the leading instability channel in the weak-coupling limit. In the vicinity of fine-tuned points such as van Hove singularities or quadratic band touchings, however, other competing channels can be induced even by infinitesimal interactions; hence, this treatment holds only away from these points [which is the case for the studied model (2)]. We first calculate the lowest-order diagrams shown in Fig. S1 in Supplemental Material [49], from which we obtain the effective interaction U_{eff}, quantifying the superconducting instabilities. The largest U_{eff} corresponds to the leading instability. U_{eff} is also a measure of the critical temperature. We note that these diagrams contain as integrands the static particle-hole susceptibility χ_{ph} and the static particle-particle susceptibility χ_{pp}. While the latter diverges at the superconducting instability, the former does not and is, hence, evaluated in order to identify the symmetries of the superconducting order parameter. The methodological steps of the method are explained in detail in Supplemental Material [49]; we emphasize that the method is asymptotically exact only in the limit of infinitesimal interactions, hence leading to a potentially limited predictive power beyond the weak-coupling regime. For all WCRG calculations, we choose between 228 and 312 patching points on the FS and an adaptive integration grid [55], with effectively $(640)^2$ points in the Brillouin zone [61].

Results.—For the particular band structure of Sn/Si(111), at $U_1 = 0$, we find a leading chiral d-wave instability only in a comparably small range of dopings $0.9 \leq n \leq 0.95$ [see Figs. 2(a) and 2(b)]. Instead, for $0.95 < n < 1$ we find a close to degeneracy of d-wave and f-wave solutions (E_2 and B_2 irreps). For electron doping $n > 1$, the f-wave instability is most favorable. Considering hole dopings $n < 0.9$, chiral d-wave and chiral p-wave solutions are close to degenerate (E_2 and E_1 irreps). The amplitude of the superconducting form factor U_{eff} is shown in Fig. 2(c) and reveals the aforementioned competition between the different pairing channels (the symmetry of the form factor is shown in Fig. S2 [49]). This competition between odd- (f- and p-wave) and even-parity pairing (d-wave) is *a priori* unexpected, as most often chiral d-wave is the leading instability for hexagonal tight-binding models [40,42–46]. For comparison, in Figs. 1(b) and 1(c) we display the FSs of the Sn/Si(111) band and of an isotropic nearest-neighbor triangular lattice, respectively. Pronounced peaks in the bare susceptibility for the latter are suppressed when switching to Sn/Si(111) where the FS is warped due to longer-ranged hoppings. Thus, even without the inclusion of U_1, we can see why singlet pairing is less favorable than in other hexagonal systems.

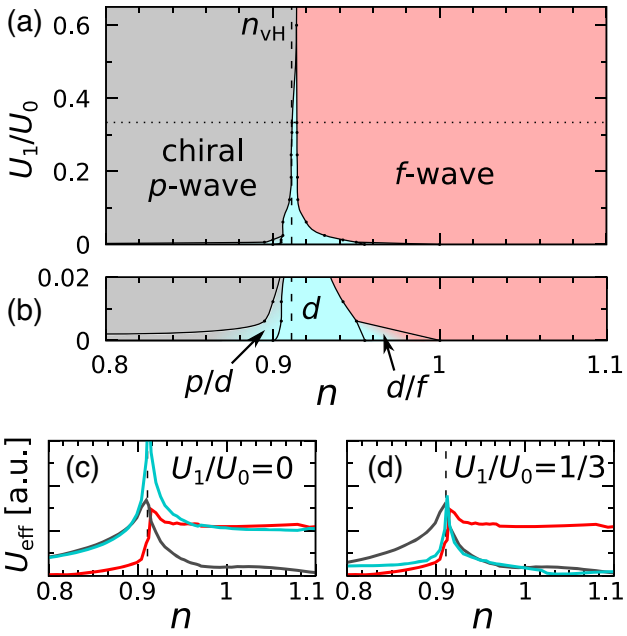

FIG. 2. (a) Weak-coupling phase diagram as a function of nonlocal Coulomb interaction U_1/U_0 vs band filling n for Sn/Si(111). For band fillings above the van Hove singularity, triplet superconductivity with $f_{y(3x^2-y^2)}$-wave symmetry (B_2 irrep in red) is found. For fillings below van Hove (corresponding to hole dopings larger than 8.5%), chiral triplet superconductivity with $p_x + ip_y$-wave symmetry (E_1 irrep in gray) is present. (b) Enlargement of the phase diagram with very small nonlocal Coulomb interactions reveals a small area with chiral d-wave (E_2 irrep in cyan) pairing as well as regions where d-wave is degenerate with f-wave (electron-doped) and with p-wave (hole-doped). (c) Effective interaction U_{eff} for $U_1 = 0$: p- and d-wave pairings ($n < n_{\text{vH}}$) and f- and d-wave pairings ($n > n_{\text{vH}}$) are degenerate. (d) For significant U_1/U_0 as assumed for Sn/Si(111), d-wave pairing is suppressed, leading to chiral p-wave and f-wave superconductivity.

Motivated by previous work [29,30], we assume that nonlocal Coulomb interactions—modeled via nearest-neighbor repulsion U_1—are crucial for boron-doped Sn/Si(111). The presence of U_1 further suppresses chiral d-wave and leaves odd-parity f-wave pairing ($n > 0.91$) or chiral p-wave pairing ($n < 0.91$) as the leading instability [see Fig. 2(a) for $U_1/U_0 = 1/3$ and Fig. S2 in Supplemental Material [49] for $U_1/U_0 = 1/2$]. The suppression of chiral d-wave also leads to a significant energetic gap between the leading and the first subleading instability [see Fig. 2(d)], indicating the stability of the superconducting ground state with respect to small perturbations as well as finite Coulomb interactions. As a central result, we identify sufficiently hole-doped Sn/Si(111) as a topological superconductor stabilized by nonlocal Coulomb repulsion.

We complement our WCRG analysis by numerical FRG calculations based on two key approximations: (i) neglecting the one-particle irreducible (1PI) three-particle vertex function and (ii) a Fermi surface-based discretization of the 1PI two-particle vertex. Since all details of the derivation and limits of the scheme have been extensively reviewed [47–49], we focus on the key results of our calculation in the following and present a concise summary of our approach in Supplemental Material [49] including Refs. [62,63]. As a diagrammatic resummation scheme that includes leading-order vertex corrections and treats all two-particle interactions on equal footing, we use the FRG to assess the stability of our WCRG results toward an increase in coupling strength from weak to intermediate coupling. Moreover, the FRG allows us to rule out other competing many-body instabilities due to its unbiased treatment of the particle-hole and particle-particle channels. For $U_0 = 5t_1$ and $U_1 = 0$, d-wave becomes the dominant instability within FRG. This is in line with previous FRG studies: For a Fermi-ology such as given by Sn/Si(111), sufficient on-site Hubbard coupling strength tends to give preference to singlet pairing. In line with WCRG, however, the addition of U_1 indeed can tilt the balance in favor of triplet pairing, as we observe the d-wave state in FRG start to destabilize at finite U_1 in favor of f-wave pairing at half filling $n \approx 1$ and p-wave pairing at $n < 0.75$. Figure 3 depicts a representative FRG flow diagram for $U_1/U_0 = 1/2$ where the p-wave instability turns out to dominate and to eventually yield a preferred chiral p-wave order parameter in order to maximize condensation energy. FRG further reveals that competing many-body instabilities such as spin and charge density waves and a nematic phase are subleading compared to superconductivity (Fig. 3). Note that if the interaction scale is increased even further within FRG, which would likely be out of the scope of Sn/Si(111), density wave instabilities start to become competitive to the superconducting instability. In total, aside from constraining the preferred doping regime a bit further, WCRG and FRG confirm the propensity of triplet pairing in Sn/Si(111), which, in particular, turns out to be strong by comparison to previous models studied within FRG.

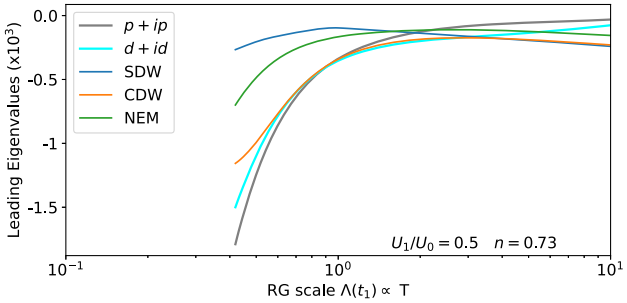

FIG. 3. Leading eigenvalues of the effective two-particle vertex, as a function of Λ, for superconducting, charge and spin density wave (CDW and SDW, respectively), and nematic (NEM) instabilities. Λ is the FRG cutoff energy, which is proportional to the temperature. The most negative eigenvalue corresponds to the leading instability. The chiral triplet $p + ip$ ordering dominates over all other ordering tendencies at low temperatures. Its strongest competitor is chiral $d + id$-wave pairing.

Discussion.—The FS of the band structure of Sn/Si(111) is warped due to the longer-ranged hoppings, which leads to a competition between singlet d-wave and triplet p-wave instabilities. The key for stabilizing triplet p-wave superconductivity, however, is the nonlocal Coulomb interaction U_1. When transforming U_1 to momentum space, it can be decoupled into contributions associated with the different irreps. They include p- (E_1 irrep) and d-wave (E_2 irrep) but not the f-wave (B_2 irrep) form factors. While this explains why the f-wave solution in Figs. 2(c) and 2(d) is not affected by U_1, one would expect p- and d-wave states to be equally affected by U_1 from this analysis. Representative form factors shown in Fig. S2 [49] reveal, however, that the p-wave instability has additional nodes. That is the reason why such an "extended" p wave is hardly affected by U_1, in contrast to the conventional d-wave state [see Figs. 2(c) and 2(d)]. We stress that an extended p wave leads to fully gapped topological superconductivity just like the ordinary p-wave state.

Single layers of ordered metal atoms such as Pb and In on Si(111) offer themselves as interesting platforms for conventional electron-phonon mediated superconductivity up to 3 K [64,65]. We have calculated the electron-phonon coupling for Sn/Si(111), leading to an estimate of $\lambda = 0.07$. This value of λ is deeply in the weak-coupling regime and far from the value of $\lambda \sim 1$ typical of high-T_c electron-phonon coupling-mediated superconductors. Details have been delegated to Supplemental Material [49] including Refs. [66–69]. Moreover, the experimentally observed antiferromagnetic order for the undoped system [33] hints at an unconventional pairing mechanism. Our work thus propounds a purely unconventional scenario, where superconductivity emerges upon hole doping of a Mott insulating phase.

In this work, we have neglected the role of spin-orbit coupling (SOC). LDA calculations including SOC show

that its effect is rather small. In addition, small to modest contributions of SOC give rise to only some mild mixing of the different pairing channels [70], and the conclusions regarding the dominant superconducting instability will not change.

Our Letter emphasizes the role of nonlocal Coulomb interactions in order to stabilize spin-triplet pairing. The same had been previously observed for one-band Hubbard models on the square, triangular, and honeycomb lattice [43,55]. In a recent paper [71], it was found for a Rashba-Hubbard model on the square lattice that the inclusion of U_1 leads to an enhancement of triplet pairing.

Another group-IV adsorbate, which features essentially the same band structure as Sn/Si(111) and is also believed to have significant nonlocal Coulomb interactions, is Pb/Si(111) [29,30,42]; it was estimated that $U_1/U_0 = 3/5$, and, according to Fig. 2(a), we find the same pairing instabilities as for Sn/Si(111). Given the experimental efforts to dope Pb/Si(111), this might be another promising candidate to search for spin-triplet pairing.

Conclusion.—We have shown theoretically that the recently discovered superconductivity in Sn/Si(111) could realize the elusive case of spin-triplet pairing. In contrast to most scenarios on hexagonal lattices where chiral d-wave dominates, we show that the band structure of Sn/Si(111) leads to a competition between d-wave and spin-triplet pairings. We further argue that nonlocal Coulomb interactions are non-negligible in Sn/Si(111); including them suppresses the chiral d-wave state. For moderate hole dopings, we find f-wave pairing; most interestingly, hole dopings larger than 8.5%, as achieved in recent experiments, stabilize the archetypal topologically nontrivial $p + ip$-wave state. Our weak-coupling analysis is backed up by intermediate-coupling FRG simulations which further substantiate our results. Given the simple chemical and electronic structure of Sn/Si(111) and other adatom lattices on semiconductor substrates, they might provide the cleanest platform for studying (topological) superconductivity emerging from a doped Mott insulator in the future.

We acknowledge discussions with R. Claessen, J. Schäfer, F. Adler, M. Laubach, P. R. Brydon, T. L. Schmidt, and J. Makler. This work is funded by the Australian Research Council through Grants No. FT180100211 and No. DP200101118, by the Deutsche Forschungsgemeinschaft (DFG, German Research Foundation) through Project-ID No. 258499086-SFB 1170, and by the Würzburg-Dresden Cluster of Excellence on Complexity and Topology in Quantum Matter ct.qmat Project-ID No. 390858490-EXC 2147. The research leading to these results has received funding from the European Unions Horizon 2020 research and innovation program under the Marie Sklodowska-Curie Grant Agreement No. 897276. We gratefully acknowledge the HPC facility Spartan hosted at the University of Melbourne and the Gauss Centre for Supercomputing e.V. for funding this project by providing computing time on the GCS Supercomputer SuperMUC at Leibniz Supercomputing Centre. The Flatiron Institute is a division of the Simons Foundation.

[1] J. G. Bednorz and K. A. Müller, Z. Phys. B **64**, 189 (1986).
[2] G. R. Stewart, Rev. Mod. Phys. **83**, 1589 (2011).
[3] I. I. Mazin and J. Schmalian, Physica (Amsterdam) **469C**, 614 (2009).
[4] M. Sato and Y. Ando, Rep. Prog. Phys. **80**, 076501 (2017).
[5] C. Kallin and J. Berlinsky, Rep. Prog. Phys. **79**, 054502 (2016).
[6] Y. Tanaka, M. Sato, and N. Nagaosa, J. Phys. Soc. Jpn. **81**, 011013 (2012).
[7] M. Smidman, M. B. Salamon, H. Q. Yuan, and D. F. Agterberg, Rep. Prog. Phys. **80**, 036501 (2017).
[8] D. A. Ivanov, Phys. Rev. Lett. **86**, 268 (2001).
[9] C. Nayak, S. H. Simon, A. Stern, M. Freedman, and S. Das Sarma, Rev. Mod. Phys. **80**, 1083 (2008).
[10] R. M. Lutchyn, J. D. Sau, and S. Das Sarma, Phys. Rev. Lett. **105**, 077001 (2010).
[11] Y. Oreg, G. Refael, and F. von Oppen, Phys. Rev. Lett. **105**, 177002 (2010).
[12] V. Mourik, K. Zuo, S. M. Frolov, S. R. Plissard, E. P. A. M. Bakkers, and L. P. Kouwenhoven, Science **336**, 1003 (2012).
[13] S. Nadj-Perge, I. K. Drozdov, J. Li, H. Chen, S. Jeon, J. Seo, A. H. MacDonald, B. A. Bernevig, and A. Yazdani, Science **346**, 602 (2014).
[14] A. Palacio-Morales, E. Mascot, S. Cocklin, H. Kim, S. Rachel, D. K. Morr, and R. Wiesendanger, Sci. Adv. **5**, eaav6600 (2019).
[15] E. Bauer, G. Hilscher, H. Michor, C. Paul, E. W. Scheidt, A. Gribanov, Y. Seropegin, H. Noël, M. Sigrist, and P. Rogl, Phys. Rev. Lett. **92**, 027003 (2004).
[16] Y. Yanase and M. Sigrist, J. Phys. Soc. Jpn. **77**, 124711 (2008).
[17] Y. S. Hor, A. J. Williams, J. G. Checkelsky, P. Roushan, J. Seo, Q. Xu, H. W. Zandbergen, A. Yazdani, N. P. Ong, and R. J. Cava, Phys. Rev. Lett. **104**, 057001 (2010).
[18] S. Sasaki, M. Kriener, K. Segawa, K. Yada, Y. Tanaka, M. Sato, and Y. Ando, Phys. Rev. Lett. **107**, 217001 (2011).
[19] P. Zhang, K. Yaji, T. Hashimoto, Y. Ota, T. Kondo, K. Okazaki, Z. Wang, J. Wen, G. D. Gu, H. Ding, and S. Shin, Science **360**, 182 (2018).
[20] J. D. Rameau, N. Zaki, G. D. Gu, P. D. Johnson, and M. Weinert, Phys. Rev. B **99**, 205117 (2019).
[21] Z. Wang, J. O. Rodriguez, L. Jiao, S. Howard, M. Graham, G. D. Gu, T. L. Hughes, D. K. Morr, and V. Madhavan, Science **367**, 104 (2020).
[22] S. Ran, C. Eckberg, Q.-P. Ding, Y. Furukawa, T. Metz, S. R. Saha, I.-L. Liu, M. Zic, H. Kim, J. Paglione, and N. P. Butch, Science **365**, 684 (2019).
[23] A. P. Mackenzie and Y. Maeno, Rev. Mod. Phys. **75**, 657 (2003).
[24] A. Pustogow *et al.*, Nature (London) **574**, 72 (2019).
[25] S. A. Kivelson, A. C. Yuan, B. J. Ramshaw, and R. Thomale, npj Quantum Matter. **5**, 43 (2020).

[26] H. G. Suh, H. Menke, P. M. R. Brydon, C. Timm, A. Ramires, and D. F. Agterberg, Phys. Rev. Research **2**, 032023(R) (2020).

[27] S. Ghosh, A. Shekhter, F. Jerzembeck, N. Kikugawa, D. A. Sokolov, M. Brando, A. P. Mackenzie, C. W. Hicks, and B. J. Ramshaw, Nat. Phys. **17**, 199 (2021).

[28] R. Cortés, A. Tejeda, J. Lobo-Checa, C. Didiot, B. Kierren, D. Malterre, J. Merino, F. Flores, E. G. Michel, and A. Mascaraque, Phys. Rev. B **88**, 125113 (2013).

[29] P. Hansmann, T. Ayral, L. Vaugier, P. Werner, and S. Biermann, Phys. Rev. Lett. **110**, 166401 (2013).

[30] F. Adler, S. Rachel, M. Laubach, J. Maklar, A. Fleszar, J. Schäfer, and R. Claessen, Phys. Rev. Lett. **123**, 086401 (2019).

[31] D. I. Badrtdinov, S. A. Nikolaev, M. I. Katsnelson, and V. V. Mazurenko, Phys. Rev. B **94**, 224418 (2016).

[32] C. Tresca *et al.*, Phys. Rev. Lett. **120**, 196402 (2018).

[33] G. Li, P. Höpfner, J. Schäfer, C. Blumenstein, S. Meyer, A. Bostwick, E. Rotenberg, R. Claessen, and W. Hanke, Nat. Commun. **4**, 1620 (2013).

[34] J.-H. Lee, X.-Y. Ren, Y. Jia, and J.-H. Cho, Phys. Rev. B **90**, 125439 (2014).

[35] F. Ming, S. Johnston, D. Mulugeta, T. S. Smith, P. Vilmercati, G. Lee, T. A. Maier, P. C. Snijders, and H. H. Weitering, Phys. Rev. Lett. **119**, 266802 (2017).

[36] X. Wu, F. Ming, T. S. Smith, G. Liu, F. Ye, K. Wang, S. Johnston, and H. H. Weitering, Phys. Rev. Lett. **125**, 117001 (2020).

[37] P. A. Lee, N. Nagaosa, and X.-G. Wen, Rev. Mod. Phys. **78**, 17 (2006).

[38] K. Takada, H. Sakurai, E. Takayama-Muromachi, F. Izumi, R. A. Dilanian, and T. Sasaki, Nature (London) **422**, 53 (2003).

[39] R. E. Schaak, T. Klimczuk, M. L. Foo, and R. J. Cava, Nature (London) **424**, 527 (2003).

[40] A. M. Black-Schaffer and C. Honerkamp, J. Phys. Condens. Matter **26**, 423201 (2014).

[41] X. Gong, M. Kargarian, A. Stern, D. Yue, H. Zhou, X. Jin, V. M. Galitski, V. M. Yakovenko, and J. Xia, Sci. Adv. **3**, e1602579 (2017).

[42] X. Cao, T. Ayral, Z. Zhong, O. Parcollet, D. Manske, and P. Hansmann, Phys. Rev. B **97**, 155145 (2018).

[43] X. Wu, M. Fink, W. Hanke, R. Thomale, and D. Di Sante, Phys. Rev. B **100**, 041117(R) (2019).

[44] R. Nandkishore, R. Thomale, and A. V. Chubukov, Phys. Rev. B **89**, 144501 (2014).

[45] M. H. Fischer, T. Neupert, C. Platt, A. P. Schnyder, W. Hanke, J. Goryo, R. Thomale, and M. Sigrist, Phys. Rev. B **89**, 020509(R) (2014).

[46] D. Di Sante, X. Wu, M. Fink, W. Hanke, and R. Thomale, Phys. Rev. B **99**, 201106(R) (2019).

[47] W. Metzner, M. Salmhofer, C. Honerkamp, V. Meden, and K. Schönhammer, Rev. Mod. Phys. **84**, 299 (2012).

[48] C. Platt, W. Hanke, and R. Thomale, Adv. Phys. **62**, 453 (2013).

[49] See Supplemental Material at http://link.aps.org/supplemental/10.1103/PhysRevLett.128.167002 for details about the WCRG and FRG methods.

[50] See supplemental material of Ref. [30] and, in particular, Sec. IV therein.

[51] Previous works assumed values for U_0 of the order of $\sim 20t_1$ [29,30] which is a regime where we do not expect superconductivity; thus, we consider considerably weaker on-site interactions, while we assume the ratio U_1/U_0 to be unchanged.

[52] S. Raghu, S. A. Kivelson, and D. J. Scalapino, Phys. Rev. B **81**, 224505 (2010).

[53] S. Raghu and S. A. Kivelson, Phys. Rev. B **83**, 094518 (2011).

[54] S. Raghu, E. Berg, A. V. Chubukov, and S. A. Kivelson, Phys. Rev. B **85**, 024516 (2012).

[55] S. Wolf, T. L. Schmidt, and S. Rachel, Phys. Rev. B **98**, 174515 (2018).

[56] T. Scaffidi, *Weak-Coupling Theory of Topological Superconductivity* (Springer Theses, Springer International Publishing AG, New York, 2017), ISBN: 978-3-319-62867-7.

[57] M. L. Kiesel and R. Thomale, Phys. Rev. B **86**, 121105(R) (2012).

[58] W. Cho, R. Thomale, S. Raghu, and S. A. Kivelson, Phys. Rev. B **88**, 064505 (2013).

[59] W. Kohn and J. M. Luttinger, Phys. Rev. Lett. **15**, 524 (1965).

[60] R. Shankar, Rev. Mod. Phys. **66**, 129 (1994).

[61] We repeated for selected parameter points the calculations with up to 600 patching points on the FS and for an integration grid with up to $(1280)^2$ points in the Brillouin zone; the results did not change, proving that the chosen resolution is sufficient.

[62] M. Salmhofer and C. Honerkamp, Prog. Theor. Phys. **105**, 1 (2001).

[63] N. Dupuis, L. Canet, A. Eichhorn, W. Metzner, J. M. Pawlowski, M. Tissier, and N. Wschebor, Phys. Rep. **910**, 1 (2021).

[64] T. Zhang, P. Cheng, W. J. Li *et al.*, Nat. Phys. **6**, 104 (2010).

[65] J. Noffsinger and M. L. Cohen, Solid State Commun. **151**, 421 (2011).

[66] G. Kresse and J. Furthmüller, Phys. Rev. B **54**, 11169 (1996).

[67] A. Togo and I. Tanaka, Scr. Mater. **108**, 1 (2015).

[68] F. S. Khan and P. B. Allen, Phys. Rev. B **29**, 3341 (1984).

[69] J. M. An and W. E. Pickett, Phys. Rev. Lett. **86**, 4366 (2001).

[70] S. Wolf and S. Rachel, Phys. Rev. B **102**, 174512 (2020).

[71] R. Ghadimi, M. Kargarian, and S. A. Jafari, Phys. Rev. B **99**, 115122 (2019).